ACS SYMPOSIUM SERIES

Interactions of Food Proteins

Nicholas Parris, EDITOR
Robert Barford, EDITOR
U.S. Department of Agriculture

Developed from a symposium sponsored
by the 1989 International Chemical Congress
of Pacific Basin Societies,
Honolulu, Hawaii,
December 17–22, 1989

Chapter 13

Quaternary Structural Changes of Bovine Casein by Small-Angle X-ray Scattering

Effect of Genetic Variation

T. F. Kumosinski, H. Pessen, E. M. Brown, L. T. Kakalis, and H. M. Farrell, Jr.

Eastern Regional Research Center, Agricultural Research Service, U.S. Department of Agriculture, Philadelphia, PA 19118

Milks containing the A or B genetic variants of α_{s1}-casein have markedly different physical properties (solubility, heat stability). When examined by small-angle X-ray scattering (SAXS), whole caseins, either A or B, as submicelles (without Ca^{2+}) behaved as inhomogeneous spheres with two concentric regions; the inner (more electron dense) region displayed protein-protein inter- actions, the outer region, high hydration. Upon addition of Ca^{2+}, casein of both variants, while retaining its submicellar hydration and structure was packed into colloidal micelles at ratios of 3:1 for B, and 6:1 for A. Tightly bound water (by ^2H NMR relaxation) was only a fraction of total water (by SAXS): thus both micelles and submicelles contained trapped water. For both micelles and submicelles, similar dynamic motions were observed by ^{13}C NMR. Open penetrable 3-D structures of α_{s1}- and κ-caseins were predicted by energy minimization. All results support a model featuring micelles composed of submicelles which exhibit high mobility accounting for the known diffusion of enzymes and cosolutes throughout the casein micelle.

Whole casein occurs in bovine milk as a colloidal calcium-phosphate-containing protein complex, commonly called the casein micelle. The micellar structure is disrupted by the removal of calcium, resulting in noncolloidal protein complexes called submicelles (1). These submicelles consist of four proteins, α_{s1}-, α_{s2}-, β- and κ-casein, in the approximate ratios of 4:1:4:1 (2). All are phosphorylated to various extents and have an average monomer molecular weight of 23,000 (3). Isolated casein fractions exhibit varying degrees of self-association which are mostly hydro- phobically driven (1). The nature of tertiary and quaternary structures of native caseins in mixed association has received little attention. However, there is hydrodynamic evidence that, in the absence of calcium, casein monomers associate to form aggregates, submicelles, with a maximum Stokes radius of 9.4 nm (4).

Upon the addition of calcium, these hydrophobically stabilized casein submicelles further self-associate to colloidal micelles with average radii of 65 nm. The formation of micelles is thought to occur via calcium-protein side-chain salt bridges (1,4). The exact supramolecular structure of the casein micelle remains a topic of controversy. Proposed models of the casein micelle include: a micelle composed of discrete submicelles (3); a loose, porous gel structure (5); and a newer model of a homogeneous sphere with a "hairy" outer layer (6).

X-ray crystallography is generally the technique of choice for the elucidation of protein structure. However, for proteins such as casein, which do not crystallize, valuable molecular information may be extracted by the companion technique of small-angle X-ray scattering

(SAXS). This technique which measures the intensity of scattering produced by the electrons of the solute can yield valuable information including degree of hydration, radius of gyration and molecular weight (7).

SAXS was undertaken on whole bovine casein from two distinct genetic lines (α_{s1}-caseins A and B), first in the absence of calcium to describe the nature of the limiting polymer structure of these two whole caseins (submicellar structures) and second, in the presence of calcium, to determine if the colloidal micelle consists of discrete submicellar particles with a particular packing structure or of a nonspecific, unordered, gel-like structure. Since milks containing these two genetic variants differ in their physical properties (8), information on the molecular basis for these differences could be assessed as well. The results of these studies are correlated with previous studies on micelles and submicelles using ^2H NMR relaxation and ^{13}C NMR spectroscopy of the caseins.

Materials and Methods

Sample Preparation. Whole sodium caseinate from the milks of two individually selected cows was prepared as described previously (9). These caseins were of the genotypes (α_{s1}-AA, β-AA, κ-AA) and (α_{s1}-BB, β-AA, κ-BB) (10). Casein micelles were prepared by the addition of $CaCl_2$ (final concentration 10 mM) to a solution of lyophilized caseinate in PIPES-KCl buffer (25 mM piperazine-N-N'-bis (2-ethanesulfonic acid), pH 6.75, made to be 80mM in KCl) (9). For the preparation of submicelles the $CaCl_2$ was replaced by additional KCl (30 mM to match the ionic strength of the $CaCl_2$).

SAXS Measurements and Data Analysis. The measurement of SAXS and evaluation of data were as described previously (9) using the Cu-K_α doublet at 0.154 nm. For data evaluation, the partial specific volume $\bar{v}$ and number of electrons per gram of particle were calculated from the amino acid composition (11). The computer program of Lake (12) was used to deconvolute slit-smeared curves. All data were fitted to multiple Gaussian functions by the use of a Gauss-Newton nonlinear-regression computer program developed at this laboratory (9). Lowest root mean square variation and random residuals were used as criteria for the number of Gaussians used.

NMR Measurements. Proton-decoupled, natural abundance ^{13}C (100.5 MHz) NMR measurements were carried out with a JEOL GX-400 multinuclear spectrometer. (Reference to brand or firm name here and in the following does not constitute endorsement by the U.S. Department of Agriculture over others of a similar nature not mentioned.) Generally, 240 mg of lyophilized caseinate containing α_{s1}-B were dissolved in 4 ml D_2O (6.0 % w/v), containing KCl for casein submicelles or KCl-$CaCl_2$ for casein micelles, together with 0.3 mg/ml sodium 2,2-dimethyl-2-silapentane-5 sulfonate (DSS) as an internal chemical shift standard. The 90^o pulsewidth was 24 ms, the spectral width 25 kHz, the acquisition time 0.65 s and a 32K point time-domain array was used for storing the data. T_1 values were measured by inversion-recovery (13). Approximately 30 min were allowed for each sample to reach thermal equilibrium in the magnet before data acquisition. The probe temperature was controlled ($\pm 0.5^oC$) by means of a thermostated dry nitrogen current.

Molecular Modeling. Three-dimensional (3D) representations of casein monomers were constructed using Sybyl-Mendel molecular modeling programs with Evans and Sutherland hardware. Selection of appropriate conformation states for the individual amino acid residues was accomplished by comparing the results of sequence-based predictive techniques (14,15) with available spectroscopic data (16,17).

Results and Discussion

Submicelles. The SAXS data were analyzed by nonlinear regression and fitted by the sum of two Gaussian functions. For both genetic variants (A and B), these data were interpreted by means of a model in which the particle has two regions of different electron densities with the

same scattering center. In this model, the scattered amplitudes rather than the intensities of the two regions must be added because of interference effects of the scattered radiation. Molecular and structural parameters for the two caseins under submicellar conditions were evaluated using equations and notation developed by Luzzati *et al.* (18,19). These parameters are listed in Tables I and II where subscripts C and L refer to parameters for the higher (core) and lower (shell or loose) electron density regions, respectively, while subscript 2 refers to the particle including both regions.

Variant B. The molecular weight, M_2, found for the total submicellar particle containing α_{s1}-B casein, the more prevalent variant, was 285,000 ± 14,600. Both M_2 and k, the mass fraction of the denser or "core" region, were independent of protein concentration, ruling out an explanation of the multiple Gaussian character of the scattering as due to extreme particle size polydispersity (20). Extreme particle asymmetry (e.g., rods) can be ruled out from electron-microscopic, hydrodynamic, and light scattering evidence indicating approximately spherical particles (1,21). Hence the molecular parameters given in Table I are a measure of the limiting aggregate of the hydrophobically driven mixed self-association of the whole caseins in the absence of calcium. The molecular weight of this limiting polymer (M_2 = 285,000) is consistent with the 200,000 to 300,000 values found by a variety of techniques (21,22).

Table I. Molecular parameters of variants A and B (Desmeared SAXS)

Parameter	Submicelle		Micelle	
	A	B	A	B
M	-------	-------	2,090,000 ± 500,000	882,000 ± 28,000
k2	-------	-------	0.167 ± 0.038	0.308 ± 0.005
P#			6.0:1	3.2:1
M_2	312,000 ±19,000	285,000 ± 14,600	350,000 ± 28,000	276,000 ± 18,000
k	0.262 ± 0.009	0.212 ± 0.028	0.166 ± 0.010	0.216 ± 0.003
M_C	81,700 ± 4,600	60,000 ± 5,600	65,100 ± 1,900	56,400 ± 3,700
M_L	231,000 ± 15,000	225,000 ± 18,500	289,000 ± 30,000	220,000 ± 18,700
$\delta\rho^a$	-------	-------	9.3± 0.9	8.0 ± 0.4
$\delta\rho_2$	10.7 ± 0.6	9.9 ± 0.4	8.4 ± 0.4	7.3 ± 0.5
$\delta\rho_C$	18.4 ± 0.8	14.8 ± 1.4	13.4 ± 0.2	12.8 ± 0.7
$\delta\rho_L$	8.1 ± 0.4	8.5 ± 0.3	7.8 ± 0.5	5.7 ± 0.3
H^b	-------	-------	6.71 ± 0.63	7.92 ± 0.42
H_2	5.74 ± 0.27	6.31 ± 0.30	7.51 ± 0.34	8.98 ± 0.44
H_C	3.05 ± 0.17	3.97 ± 0.48	4.45 ± 0.08	4.70 ± 0.31
H_L	7.88 ± 0.40	7.41 ± 0.30	8.68 ± 0.56	11.44 ± 0.58

Values are averages for three concentrations. Units are [a] e^-/nm^3, and [b] $g_{H_2O}/g_{protein}$

In the small-angle neutron-scattering study of Stothart & Cebula (22), the data were analyzed on the basis of a model consisting of a homogeneous limiting aggregate. Here, we have found a heterogeneous particle consisting of two regions of differing electron density, with the mass fraction of the higher electron density region, k, equal to 0.212 ± 0.028. This

core region, moreover, has an electron density difference, $\Delta\rho_C$ of 14.8 ± 1.4 e^-/nm^3, a hydration, H_C, of 3.97 ± 0.48 g water/g protein, and a molecular weight, M_C, of 60,000 ± 5,600 (Table I). The region of higher electron density most likely results from the intermolecular hydrophobically driven self-association of casein monomer units (1); the hydrophobic inner core would be surrounded by a less electron-dense region (a loose or shell area) presumably consisting mainly of hydrophilic groups (23,24). The hydration formally ascribed to the core region is likely to be a characteristic of the packing density (25,26) of the hydrophobic side chains rather than any actual amount of water "bound" within this region. Our own research (27) using ^2H NMR relaxation measurements in D_20 showed that isotropically bound water associated with submicelles occurs with an average rotational correlation time of 38 ns, thus yielding a Stokes radius of 3.6 nm (Table III). This value is in good agreement with R_C of Table II (3.8 nm) found by SAXS. Thus, the most tightly bound water may occur at the surface of this more electron dense inner core, while water occurring outside this limit may be considered trapped or protein-influenced. Indeed, the ratio of hydration in the loose region, H_L, is 1.7 times that of the core region, H_C, for the submicelles (Table II).

Table II. Structural parameters of variants A and B (Desmeared SAXS)

Parameter	Submicelle		Micelle	
	A	B	A	B
V, nm^3	-------	-------	26,080 ± 2,390	12,720 ± 250
V2, nm^3	3,400 ± 90	3,330 ± 260	4,880 ± 130	4,440 ± 160
VC, nm^3	495± 30	467 ± 2	519 ± 2	529 ± 3
Vl, nm^3	3,300 ± 60	3,320 ± 400	4,580 ± 90	4,310 ± 20
R_2, nm	8.51 ± 0.02	8.02 ± 0.04	8.99 ± 0.01	9.06 ± 0.01
R_C, nm	3.93 ± 0.01	3.80 ± 0.01	3.93 ± 0.01	3.96 ± 0.01
R_L, nm	9.62 ± 0.03	8.82 ± 0.08	9.69 ± 0.03	10.02 ± 0.01
R_G,* nm	6.28	7.72	27.22	17.52
Dmax,* nm	15.66	19.89	83.38	51.21
(a/b)C	1.46	1.33	-------	-------
(a/b)2	2.28	1.98	-------	-------

Values are averages for three concentrations. (*) - calculated from the distance distribution.

still low when compared to compact globular proteins (20), such as lysozyme (78 e^-/nm^3), α-lactalbumin (67 e^-/nm^3), ribonuclease (71 e^-/nm^3) or riboflavin-binding protein (56 e^-/nm^3). This result emphasizes the consequences of the unique nature of the conformation of the casein polypeptide chains. Caseins have long been regarded to have little secondary structure (3); however recent evidence from Raman spectroscopy (16) suggests that whole casein in the submicellar form may have more structure than estimated from the sum of the individual casein components. Moreover, the Raman data permit the estimation of the percentage of β-turns in whole casein. Nearly 40% of the casein structure occurs in β-turns, which demonstrates that the conformation of submicellar caseins is not that of a totally random structureless coil. This finding is further supported by recent 3D molecular modeling studies

of bovine casein (28). Computer-generated 3D models of α_{s1}- and κ-caseins based on secondary structural predictions and Raman data showed a retention of β-turns during energy minimization. In addition, the overall shape and known biochemical properties (availability of proteolytic cleavage sites, disulfide geometry, and positions of phosphorylated sites) were in good agreement with published data. The 3D models are also consistent with the SAXS data since they show that the monomeric caseins have hydrophobic β-sheets which may associate to produce hydrophobic inner cores.

Variant A. The molecular weight, M_2, of the submicellar particle containing the A variant of α_{s1}-casein was 312,000 ± 19,000. Both M_2 and k, the mass fraction of the denser or "core" region, were invariant as a function of protein concentration. We find that that submicelles of α_{s1}-A, like those of the B variant, consist of two regions of differing electron density, with the mass fraction of the higher electron density region equal to 0.262 ± 0.009. This higher electron density region, moreover, has an electron density difference, $\Delta\rho_C$, of 18.4 ± 0.8 e^-/nm^3, a hydration, H_C, of 3.05 ± 0.17 g water/g protein and a molecular weight, M_C, of 81,700 ± 4,600 (see Table I).

The derived structural parameters for the α_{s1}-A casein submicelles are listed in Table II. An axial ratio for the denser region, $(a/b)_C$, of 1.46 can be calculated from V_C and R_C (18), and a value of 2.28 for the axial ratio of the total submicelle, $(a/b)_2$, from V_2 and R_2, using as a model a prolate ellipsoid of revolution. These axial ratios, like the corresponding values of 1.33 and 1.98 for the B variant, are reasonable indications that the casein submicelle deviates only moderately from spherical symmetry, as would be predicted from electron microscopy (1).

Micelles. Whether the integrity of the submicellar structure is maintained within the colloidal micelle has been a subject of much controversy (5). To address this problem, the scattering of whole casein solutions of both genetic variants with 10 mM $CaCl_2$, but without phosphate buffer to compete with the protein calcium binding sites, was studied. The SAXS data for casein micelle solutions were fitted to the sum of three Gaussians. The two Gaussians having the smaller radii of gyration constitute the contribution of the submicellar structure to the SAXS results. The third Gaussian, which has the largest radius of gyration, reflects the total number of submicellar particles within the cross-sectional SAXS scattering profile. Here, at zero angle, the intensity of the larger Gaussian contribution can be simply added to the intensity of submicellar contribution. A new parameter, k_2, the ratio of the mass of the submicelles to the total observed mass ascribable to a cross section, can be expressed in terms of the radii of gyration and the zero-angle intercepts for the three Gaussians. The packing number, the reciprocal of k_2, is the number of submicellar particles found within a micellar cross section. The meaning to be ascribed to the cross section in this context will be discussed further below. The resulting parameters for micelles of both genetic variants are listed in columns 4 and 5 of Tables I and II, where subscript 2 now designates the corresponding parameters for a submicellar particle when incorporated in the micelle, and unsubscripted parameters refer to the total cross section of the colloidal particle.

Variant B. As seen in Table I, k_2 for casein micelles of α_{s1}-B was 0.308 ± 0.005, and the packing number, its reciprocal, was 3.2. The large average radius of the micelles (65 nm) implies corresponding scattering angles too small to be experimentally accessible and therefore precludes information pertaining to the total particle. One can observe only a cross-sectional portion of the colloid, with molecular weight, M, of 882,000 ± 28,000, an electron density difference, Δρ, of 8.1 ± 0.4 e^-/nm3, a hydration, H, of 7.92 ± 0.42 g water/g protein, and a volume, V, of (12.72 ± 0.25) x $10^3/nm^3$. By contrast, molecular weights of whole casein micelles have been reported to range from 0.5 to 1 x 10^9 (21). It is clear, therefore, that of the cross-sectional parameters only the electron density difference and the hydration can be directly compared with literature values. Our result for hydration of 7.92 g water/g protein is somewhat larger than the largest value reported by small-angle neutron-

scattering (4.0 to 5.5) (22). Other reported values have ranged from 2 to 7, depending upon the method employed (5).

Studies by ^2H NMR (Table III) showed that the overall degree of tightly bound water increased nearly 2.5-fold on going from the submicellar to the micellar state. SAXS data indicate that overall hydration increases 1.4-fold, with the main increase occurring in H_L, the hydration of the loose region. The average Stokes radius of the bound water, as detected by ^2H NMR, increased to 4.29 nm in the micelle (Table III); in contrast, R_C from SAXS increased only slightly to 3.96 mm while R_L increased significantly. Thus, the isotropically bound water in the micelle most likely occurs outside of the core region, but well within the loose region. It should be noted that few secondary structural changes accompany the transitions that occur on micelle formation (16). Thus, gross conformational changes can be ruled out, although some small structural rearrangements may occur (16,17). All of these results indicate an increase in both bound and trapped water on going from the submicellar to the micellar state.

TABLE III. Hydration dynamics and geometry of casein bound water, isotropic mechanism [1]

Sample B Variant	Temperature °C	θ ns	nw gH_2O/ g protein	Radius nm
Submicelles	30	38.9	0.00652	3.64
	15	34.7	0.00824	3.05
	2	29.8	0.01201	2.55
Micelles	30	63.6	0.0165	4.29
	15	51.1	0.0225	3.48
	2	45.1	0.0282	2.93

[1]Taken from reference (27).

With regard to the electron density difference, $\Delta\rho$, this parameter remains, within error, relatively unchanged for the core region on addition of Ca^{2+}; this supports the conclusion that the internal core consists mainly of a hydrophobically rich environment. Nevertheless, the absolute electron density of this region remains, as noted above, significantly lower than in globular proteins.

The major change in electron density difference occurs for the loose region, a 30% reduction for micelles of the B variant. This is accompanied not only by an increase in hydration, H_L, but by an increase in volume, V_L. For these parameters, it appears likely that the increases are due to Ca^{2+} binding to protein electrostatic groups within this region. Moreover, the binding of Ca^{2+} occurs not only with phosphate groups but also with carboxylate groups, as shown most recently by FTIR (17). Thus, the binding of Ca^{2+} to submicelles and the subsequent transition to the micellar state does not produce more compact structures but rather more open structures. Overall, the characteristics of the submicelles appear to persist within the micelle. This conclusion is supported by recent small-angle neutron-scattering data on fresh milk micelles (29).

A note of caution is in order regarding the use of the micellar parameters, other than the hydration and electron density. As already mentioned, these do not refer to the entire particle but only to a sample portion which is restricted in size by a window of scattered intensities bounded by the lower small-angle limit of observation. They do not bear a readily defined relationship to the corresponding, but inaccessible, parameters applicable to the entire micellar particle, and therefore cannot be used to derive values for the latter. Nonetheless, the cross-sectional parameters are of value in affording an internal view of the micellar structure. The crucial comparison is between the molecular and structural parameters of the casein submicellar structure by itself (columns 2 and 3) and within the casein micelle (columns 4 and 5 of Tables I and II). Within experimental error, M_2, k, M_C and M_L are the same, V_2, V_L, R_2,

and R_L increase, and V_C increases slightly; these slight changes emphasize again that the properties of the submicelles are largely preserved within the micelle.

To ascertain the spatial arrangement of the three spheres within the observed cross-sectional scattering volume observed for α_{S1}-B, the distance distribution function, p(r), was calculated from the SAXS data for casein micelles as shown in Figure 1A. Calculation of the radius of gyration from the second moment of the p(r) data (30,31) in Figure 1A, to the maximum diameter of 51.2 nm, yielded a value of 17.52 nm.

The experimental p(r) results in Figure 1A were then compared with theoretical curves calculated by the method of Glatter (30), for various geometric models. For these, the radii of the outer and inner spheres, calculated from V_2 and V_C values of column 3 of Table II, were 10.2 and 5.0 nm, respectively. The equilateral or symmetrical triangular arrangement gave the poorest fit to the experimental data (dashed line). The Cartesian coordinates for the centers of the three inhomogeneous spheres most compatible with the experimental data were found at nonsymmetrical values of (0,0), (35,0), and (18,10) (ticked line), but a better fit resulted from changing the radius of the (0,0) sphere to 12.5 nm (solid line). In fact, a radius of gyration of 17.45 nm is calculated from the theoretical p(r) curve for this inhomogeneous, irregular, triangular structure, in excellent agreement with the value of 17.52 nm found from the experimental p(r) data. It is notable that these best-fit coordinates imply interdigitation of the "loose" regions of the three submicelles (Figure 1B).

The loose, highly solvated regions of the submicelles thus retain most of their characteristics upon incorporation into the micelle. Therefore, it seems logical to assume that these loose regions will naturally form the outermost layers of the casein micelles. This means that the micellar surface would have a porous hydrophilic outer layer occurring at depths of up to 6 nm (R_L-R_C of micelles Table II). The "hairy" micelle theory (6) calls for projecting hairs of the macropeptide of κ-casein to extend outward from the micelle over average distances of 12 nm. While κ-casein most likely predominates at the surface of casein micelles, it seems unlikely that the entire loose regions, and indeed a part of the hydrophobic core, would be made up completely of the hydrophilic κ-casein macropeptide. It would seem more logical and cautious at this juncture to ascribe the non-coalescence of casein micelle, or "stability to close approach" as it was termed by Waugh (32), to a combination of steric and electrostatic forces which occur in the loose volume element of the outermost submicelles.

In fact, this feature is not unique to casein. An outer, less electron dense, region, albeit much smaller than that of the caseins, has been calculated for the compact globular protein ribonuclease (9). Indeed, changes in the surface environment of even small globular proteins are responsible for maintenance of monomeric structure as well as aggregation and denaturation. For most enzymes and structural proteins many of their associative properties are controlled by preferential solvation or preferential binding. The basic theories for these interactions were elucidated by Arakawa and Timasheff (33,34).

Variant A. As seen in Table I, the k_2 value for casein micelles of variant A was 0.167 ± 0.038 and its packing number 6.0. The cross-sectional portion of the colloid has a molecular weight, M, of 2,090,000 ± 500,000, an electron density difference, Δρ, of 9.3 ± 0.9 e^-/nm3, a hydration, H, of 6.71 + 0.63 g water/g protein (Table I) and a volume, V, of (26.08 ± 2.39) x 10^3/nm^3 (Table II). The distribution function for variant A could not be treated as was that for variant B, though it showed two separate peaks, probably a reflection of this denser packing into micelles (6:1 in place of 3:1) (Figure 2).

The molecular (Table I) and structural (Table II) parameters for A and B show many consistent differences in both submicelles and micelles. For submicelles, the various electron density differences were somewhat higher for A than for B, and this was the case also with V_2 and V_C. The various hydrations, on the other hand, were lower for A than for B in both submicelles and micelles. On going from the submicellar to the micellar state, greater differences occurred in the micelles containing A. Here, molecular weights were substantially higher for A than B, but the various radii of gyration did not increase for micelles of A as they did for those of B.

The most striking differences observed were those in the values of k. In the submicelles of A, these were more than double those of B, while in the micelles both k_2 and k_C were far

A

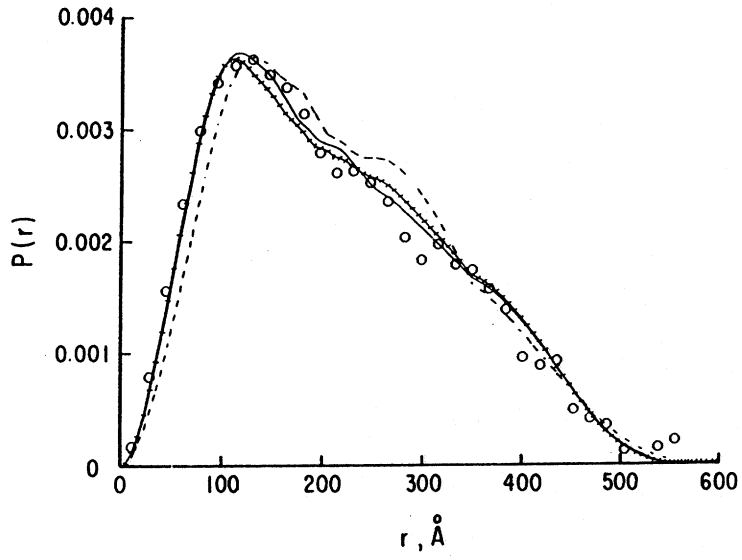

B

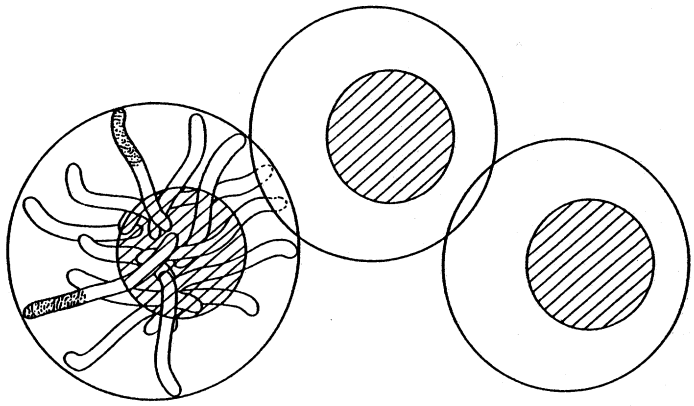

Figure 1. (A) Distance distribution of micelles. o, $p(r)$ vs r from SAXS data for micellar casein (variant B) at 16.4 mg/ml in 10 mM $CaCl_2$. Compared with theoretical curves for three inhomogeneous spheres (submicelles) all with outer radii of 10.2 nm and inner radii of 5.0 nm (+++) at (0, 0), (350, 0) , and (180, 100); (- - - -) in a symmetrical triangular arrangement ; (———) with two different outer radii at (0, 0; 12.5 nm), (350, 0; 10.2 nm), and (180, 0; 10.2 nm.) Theoretical curves were calculated by method of Glatter (30). (B) Schematic representation of submicelles in micellar cross section, corresponding to (———) in (A). Cross-hatched area, approximate region of higher concentration of hydrophobic side chains and higher electron density. In the lower left particle a few representative monomer chains are indicated.

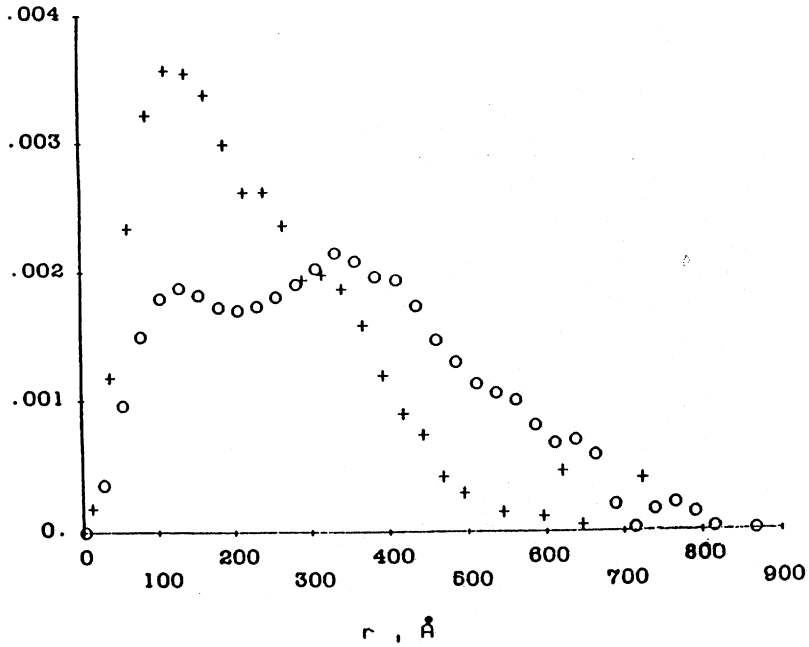

Figure 2. Distance distributions of micelles: variant A (o); variant B (+).

smaller for A than for B. These differences relate to the much higher packing number in A than in B. This larger packing number in A, as well as the larger molecular weight of the compact region and the greater elliptic eccentricity, most likely have their origins in the small but distinct differences in sequences, in calcium binding sites, and in charge distributions (35). The deletion which occurs in α_{s1}-A produces profound changes in the physical properties of the milk. The micelles are less well hydrated, and the milks have a very low heat stability (8). In addition there is a difference in overall micelle size, with micelles of A being larger than those of B (36) The high packing number disclosed by SAXS appears to be the physical basis for all of these differences in properties.

There is, however, the possibility of a completely different interpretation of the data. It could be that variant B actually does have the same packing number, 6, as A, but for reasons of interference this does not become apparent in the parameters of B. It is conceivable that the residues present in B, but absent in A, give rise to formation of a dimerlike structure, in which pairs of oppositely arranged submicelles might cause destructive interference such that half the submicelles would, in effect, remain invisible to X-rays. Only half the actual packing number (3 rather than 6) would then be observed. The differences in parameters which we found between the variants would have little part in this interpretation, but they might still be invoked to explain some of the differences in behavior of the variants. While speculative, this explanation cannot be ruled out without substantially more detailed information about casein molecular structure.

Molecular Dynamics of Casein by ^{13}C NMR. The picture presented thus far for casein micelles and submicelles is that of an open porous structure for both of these particles. The evidence supporting this feature of micelle structure comes from water binding and SAXS studies (9,27). If indeed this is the case, one would expect considerable mobility for the amino acid side chains and perhaps even for the casein backbones as well. An independent technique for studying the molecular dynamics of proteins is ^{13}C NMR.

Although the assumption of isotropic motion for protein side chains is generally an oversimplification, it may be a reasonably accurate description for immobile groups within spherical proteins and protein assemblies (such as submicelles and micelles) and can serve as a point of departure for a discussion of mobilities as detected by NMR.

Carbon-13 NMR relaxation measurements provide information concerning the mobility of chemical groups within protein molecules on the timescale of 10^{-7} to 10^{-12}s (37,38). The average rotational correlation time for backbone carbon atoms of a native protein is a reliable estimate of the correlation time for the overall tumbling of the entire protein molecule (39). Correlation times, τ_c, that characterize the overall isotropic tumbling of casein submicelles and micelles can be estimated from the Stokes radius of the particle and the viscosity of the medium. The mere observation of high-resolution ^{13}C NMR spectra (Fig. 3) for casein submicelles and micelles strongly suggests the occurrence of considerable fast local motion within these two large particles. The decrease in mobility upon micelle formation is much less than expected from the increased protein size where, in the absence of local motion, peaks would be too broad to be detected.

T_1 values of the submicelle and micelle αCH envelopes are essentially identical (390 ms at 37°C), strongly suggesting that the dynamic state of the submicelle backbones is not affected by incorporation into casein micelles. The corresponding correlation time for an isotropic rotation model (no internal motion) is approximately 8 ns (40). Consideration of a more involved model with a 10 ps internal libration at a mean angle of 20° in addition to the overall isotropic rotational tumbling (38) results in a reduction of τ_c by a factor of 2. These values (8 or 4 ns) are comparable to those of small monomeric globular proteins, well below the 56 ns expected for the overall tumbling of the 4 nm - radius submicelles.

There appears to be considerable mobility of the protein backbones within the casein submicelle. Attempts to assess the dynamic state of casein by ^1H NMR (41-43) were thwarted by the extensive spectral overlap which interfered with estimation of mobility from linewidths. The broad-featured casein ^1H NMR spectra appeared to be the result of limited spectral resolution rather than restricted molecular mobility. Indeed, proton NMR data have suggested the existence of some fast motion within casein micelles (41-43). In one study, the

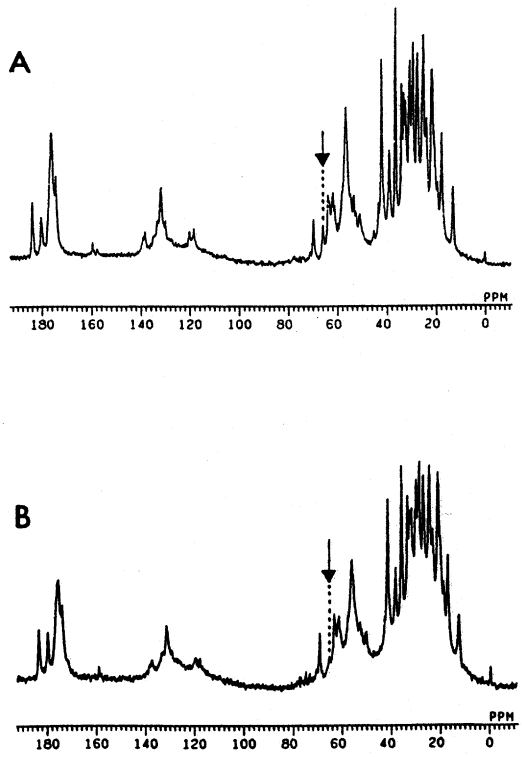

Figure 3. Natural-abundance $^{13}C\{^{1}H\}$ NMR spectra of submicelles (A) and micelles (B) of whole casein (variant B). The peak (indicated by the arrow) assigned to the βCH_2 of phosphoserine is broadened in the presence of calcium. Decreased resolution in (B) compared to (A) may result from a decrease in field homogeneity due to different magnetic susceptibilities of the micelle particle and the surrounding solution.

mobile protein regions were exclusively identified with the glycomacropeptide (GMP) segment of κ-casein, thus supporting a "hairy" micelle model, where flexible GMP chains extend into solution from the surface of rigid protein cores (41). It is unclear how such a rigid structure will at the same time be loosely packed in order to explain the ready penetration of lactose, salt and proteolytic enzymes into the micelle (1). Also, it is unlikely that the evidence of mobility in our ^{13}C NMR spectra of submicelles and micelles is solely due to the GMP which comprises less than 4% mol of whole casein and less than 0.3% protein in our samples. Other ^{1}H NMR results have indicated that only part of the observed mobility in micelles is due to κ-casein (42).

Higher mobilities are generally observed for side chain groups that are further away from the protein backbone (37-39,44). Indeed, resonances due to fast segmental motion of Lys as well as Arg and Phe (which do not occur in GMP) side chains within the casein submicelles were resolved in ^{13}C NMR spectra of both submicellar and micellar casein.

Conclusion

In summary, SAXS data for both variants argue for submicellar particles consisting of an inner, spherically symmetrical, hydrophobic, and relatively electron-dense core, surrounded by a hydrophilic and less electron-dense region, both much less dense than globular proteins, as depicted in Fig. 1A. For the casein micelles, the cross-sectional scattering volume indicates some interaction between the loose regions of adjacent submicelles. The outermost layer of the micelle is thus composed of the loose volume elements of the outer submicelles. It may be concluded that a discrete hydrophobically stabilized submicellar structure exists within the colloidal casein micelle. Such a model is supported by the high mobilities observed in ^{13}C NMR and is also in accord with the known physical and chemical properties of casein micelles including the ready diffusion of cosolutes and water.

Literature Cited

1. Schmidt, D. G. In Developments in Dairy Chemistry; Fox, P. F., Ed.; Appl. Sci., Essex, Engl,.1982; Vol. 1, p 61.
2. Davies, D. T.; Law, A. J. R. J. Dairy Res. 1980, 47, 83.
3. Farrell, H. M., Jr.; Thompson, M. P. In Calcium Binding Proteins; Thompson, M. P., Ed. CRC Press, Inc., Boca Raton, FL, 1988; Vol. 2, 117.
4. Pepper L.; Farrell, H. M., Jr. J. Dairy Sci. 1982, 65, 2259.
5. Walstra, P. J. Dairy Res. 1979, 46, 317.
6 Holt, C.; Dalgleish, D. G. J. Colloid Interface Sci. 1986, 114, 513.
7. Pessen, H.; Kumosinski, T. K.; Timasheff, S. N. Meth. Enzymol. 1973, 27, 151.
8. Thompson, M. P.; Gordon, W. G.; Boswell, R. T.; Farrell, H. M.,Jr. J. Dairy Sci. 1969, 52, 1166.
9. Kumosinski, T. F.; Pessen, H.; Farrell, H. M., Jr.; Brumberger. H. Arch. Biochem. Biophys. 1988, 266, 548.
10. Thompson, M. P. J. Dairy Sci. 1964, 47, 1261.
11. Eigel W. N.; Butler, J. E.; Ernstrom, C. A.; Farrell, H. M., Jr.; Harwalkar, V. R.; Jenness, R.; Whitney. R. McL. J. Dairy Sci. 1984, 67, 1599.
12. Lake, J. A. Acta Crystallographica 1967, 23, 191.
13. Vold, R. L.; Waugh, J. S.; Klein, M. P.; Phelps, D. E. J. Chem. Phys. 1968, 48, 3831.
14. Chou, P. Y.; Fasman, G. D. Adv. Enzymology. 1978, 47, 45.
15. Garnier, J.; Osguthorpe, D. J.; Robson B. J. Mol. Biol. 1978, 120, 97.
16. Byler, D. M.; Farrell, H. M. Jr.; Susi H. J. Dairy Sci. 1988, 71, 2622.
17. Byler, D. M.; Farrell, H. M. Jr. J. Dairy Sci. 1989, 72, 1719.
18. Luzzati, V.; Witz, J.; Nicolaieff, A. J. Mol. Biol. 1961, 3, 367.
19. Luzzati, V.; Witz, J.; Nicolaieff, A. J. Mol. Biol. 1961, 3, 379.
20. Pessen, H.; Kumosinski, T. K.; Farrell, H. M., Jr. J. Ind. Microbiol. 1988, 3, 89.
21. Schmidt, D. G.; Payens, T. A. J. In Surface and Colloid Science; Matijevic, E. Ed.; Wiley, New York, 1976; p 165.
22. Stothart, P. H.; Cebula, D. J. J. Mol. Biol. 1982, 160, 391.
23. Kuntz, I. D.; Kauzmann W. Adv. Protein Chem. 1974, 28, 239.

24. Tanford, C. In Physical Chemistry of Macromolecules; Wiley, New York, 1961;.p 236.
25. Lumry, R.; Rosenberg A. Colloques Internationaux du Centre National de la Recherche Scientifique 1975, 246, 53.
26. Richards, F. M. J. Mol. Biol. 1974, 82, 1.
27. Farrell, H. M., Jr.; Pessen, H.; Kumosinski, T. K. J. Dairy Sci. 1989 72, 562.
28. Kumosinski, T. F.; Moscow, J. J.; Brown, E. M.; Farrell, H. M., Jr. Biophys. J. 1989, 54, 333a.
29. Stothart, P. H. J. Mol. Biol. 1989, 208, 635.
30. Glatter, 0. .Acta Physica Austriaca.1980, 52, 243.
31. Pilz, I.; Glatter, 0.; Kratky, 0. Meth. Enzymol. 1979, 61, 148.
32. Waugh, D. F. In Milk Proteins; McKenzie, H. A. Ed. Academic: New York, 1971; Vol. 2, p 58.
33. Arakawa, T.; Timasheff, S. N. Biochemistry 1982, 21, 6536.
34. Arakawa, T.; Timasheff, S. N. Biochemistry 1984, 23, 5912.
35. Farrell, H. M. Jr; Kumosinski, T. K.; Pulaski, P.; Thompson, M. P. Archives Biochem. Biophys. 1988, 265, 146.
36. Dewan, R. K.; Chudgar, A.; Bloomfield, V. A.; Morr, C. V. J. Dairy Sci. 1974, 57, 394.
37. Wüthrich, K. NMR in Biological Research: Peptides and Proteins; North-Holland: Amsterdam, 1976.
38. Howarth, 0. W.; Lilley, D. M. J. Prog. NMR Spectrosc. 1978, 12, 1.
39. Richarz, R.; Nagayama, K.; Wüthrich, K. Biochemistry 1980, 19, 5189.
40. Doddrell, D.; Glushko, V.; Allerhand, A. J. Chem. Phys. 1972, 56, 3683.
41. Griffin, M. C. A.; Roberts, G. C. K. Biochem. J. 1985, 228, 273.
42. Rollema, H. S.; Brinkhuis, J. A.; Vreeman, H. J. Neth. Milk Dairy J. 1988, 42, 233.
43. Rollema, H. S.; Brinkhuis, J. A. J. Dairy Res. 1989, 56, 417.
44. Allerhand, A. Meth. Enzymol. 1979, 61, 458.

RECEIVED August 14, 1990

Reprinted from ACS Symposium Series No. 454
Interactions of Food Proteins
Nicholas Parris and Robert Barford, Editors
Published 1991 by the American Chemical Society